

Immobilized Enzymes

How to cite: *Angew. Chem. Int. Ed.* **2022**, *61*, e202117144

International Edition: doi.org/10.1002/anie.202117144

German Edition: doi.org/10.1002/ange.202117144

MOF-Hosted Enzymes for Continuous Flow Catalysis in Aqueous and Organic Solvents

Raphael Greifenstein⁺, Tim Ballweg⁺, Tawheed Hashem, Eric Gottwald, David Achauer, Frank Kirschhöfer, Michael Nusser, Gerald Brenner-Weiß, Elaheh Sedghamiz, Wolfgang Wenzel, Esther Mittmann, Kersten S. Rabe, Christof M. Niemeyer, Matthias Franzreb,* and Christof Wöll*

Abstract: Fully exploiting the potential of enzymes in cell-free biocatalysis requires stabilization of the catalytically active proteins and their integration into efficient reactor systems. Although in recent years initial steps towards the immobilization of such biomolecules in metal–organic frameworks (MOFs) have been taken, these demonstrations have been limited to batch experiments and to aqueous conditions. Here we demonstrate a MOF-based continuous flow enzyme reactor system, with high productivity and stability, which is also suitable for organic solvents. Under aqueous conditions, the stability of the enzyme was increased 30-fold, and the space–time yield exceeded that obtained with other enzyme immobilization strategies by an order of magnitude. Importantly, the infiltration of the proteins into the MOF did not require additional functionalization, thus allowing for time- and cost-efficient fabrication of the biocatalysts using label-free enzymes.

In the context of biotechnology, cell-free applications of enzymes in continuous processes has increased exponentially in recent years.^[1,2] The incorporation of immobilized enzymes in flow reactors, for example packed bed flow reactors, has gained much attention due to reduced feedback inhibition and intermediate degradation.^[3] Immobilized biocatalysts can be reused, making it more sustainable^[4,5] and used in continuous flow reactions, their space–time yield can be increased. Ideal scaffolds for hosting the catalytically active proteins should not only protect these biomolecules, but also provide the prospect of application in non-native environments and at elevated temperatures.^[6] Also, the stability against denaturing agents like acetonitrile should be improved, thus creating the prospect of applications involving organic solvents. With regard to realizing such protective scaffolds, metal–organic frameworks, MOFs, offer a rather unique spectrum of possibilities. MOFs are reticular networks obtained by coordinating organic linker molecules to metal or metal/oxo nodes, yielding porous, crystalline materials. Originally developed for applications in gas storage and separation,^[7,8] recent years have seen an increased interest with respect to innovative applications in the fields of catalysis, sensor devices, optical and electronic properties, and bioanalytical applications.^[9–11] The huge variety of geometries, linkers, and nodes available has made it possible to tailor the structure and topology of MOFs to specific needs, these reticular frameworks have already been adapted for the embedding and protection of complex bioentities such as whole cells, viruses and enzymes. With regard to the building of Enzyme@MOF, three main strategies can be distinguished (see recent reviews e.g. by Falcaro, Doonan, and co-workers):^[12–17] I) The immobilization on the surface of the MOF, II) the encapsulation by infiltration and III) the de novo encapsulation.^[18,19] Immobilization of enzymes in the voids of MOFs offers numerous advantages. In addition to protecting the protein and avoiding denaturation, the porosity of the framework materials allows one to control transport of reactants and products.^[20]

Furthermore, the separation of the catalyst from the product, a time-consuming and costly process, is substantially accelerated for MOF-embedded enzymes.^[6,21] Several proof-of-principle studies have demonstrated the potential MOF-hosted enzymes, but so far studies were mostly limited

[*] Dr. R. Greifenstein,⁺ T. Ballweg,⁺ Dr. T. Hashem, Prof. Dr. E. Gottwald, D. Achauer, F. Kirschhöfer, M. Nusser, Dr. G. Brenner-Weiß, Prof. Dr. M. Franzreb, Prof. Dr. C. Wöll
Institute of Functional Interfaces
Karlsruhe Institute of Technology
Bld. 330, Hermann-von-Helmholtz-Platz 1
76344 Eggenstein-Leopoldshafen (Germany)
E-mail: matthias.franzreb@kit.edu
christof.woell@kit.edu

Dr. E. Sedghamiz, Prof. Dr. W. Wenzel
Institute of Nanotechnology
Karlsruhe Institute of Technology
Bld. 640, Hermann-von-Helmholtz-Platz 1,
76344 Eggenstein-Leopoldshafen (Germany)

E. Mittmann, Dr. K. S. Rabe, Prof. Dr. C. M. Niemeyer
Institute for Biological Interfaces 1
Karlsruhe Institute of Technology
Bld. 601, Hermann-von-Helmholtz-Platz 1,
76344 Eggenstein-Leopoldshafen (Germany)

[†] These authors contributed equally to this work.

© 2022 The Authors. Angewandte Chemie International Edition published by Wiley-VCH GmbH. This is an open access article under the terms of the Creative Commons Attribution Non-Commercial License, which permits use, distribution and reproduction in any medium, provided the original work is properly cited and is not used for commercial purposes.

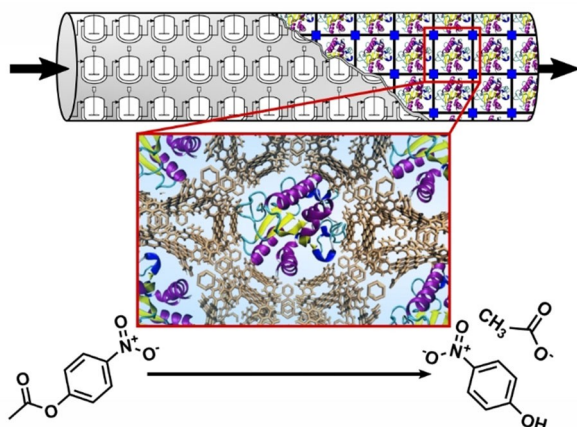
to simple batch experiments.^[22–24] Continuous-flow experiments as required for technologically relevant applications have not yet been reported for enzymes infiltrated in MOF systems. Tian et al. reported a continuous flow reactor filled with MOF coated micelles containing the enzyme CALB.^[25]

In other catalytic applications of MOFs,^[26,27] continuous-flow, packed-bed reactors^[28,29] showed substantial differences to batch experiments. Therefore, investigating Enzyme@MOF systems in a flow reactor is a crucial next step towards real world applications.

Here we report the first successful fabrication, operation in non-aqueous environments, and thorough analysis of a continuous flow reactor using single enzymes hosted within individual MOF pores (see Scheme 1). More specifically, we describe the continuous, straightforward infiltration of the esterase EST2 obtained from the thermophilic organism *Alicyclobacillus acidocaldarius* (AaEST2)^[30,31] (EC 3.1.1.1) into the pores of MOF NU-1000.^[32] The Enzyme@MOF reactor was integrated in a HPLC system equipped with state-of-the-art online analytics. With different concentrations of the substrate 4-nitrophenyl acetate and flow rates up to 1 mL min^{-1} , space–time yields (STY) of $1432 \text{ g L}^{-1} \text{ h}^{-1}$ were achieved. This is a record value, 10-times larger than the STY of enzyme reactors using other immobilization strategies.^[33,34]

The basis for our experiments is the activated MOF NU-1000. Previously, it was reported that successful synthesis of this particular MOF depends on the synthesis conditions.^[35] On the basis of the SEM-results (see Figure S4B, only hexagonal rods with smooth surfaces) and the analysis of the XRD data, we conclude that the material used here is exclusively NU-1000.^[35,36]

To investigate loading of the MOF NU-1000 with an enzyme, the recombinant esterase AaEST2 (molecular weight of 35 kDa) was purified to least 98 % (see Figure S5) and then loaded into the MOF by simply immersing the NU-1000 powder into Tris-buffered solutions containing variable amounts of AaEST2. Figure 1 shows a pronounced decrease of the esterase concentration in the supernatant as a function of contact time with the NU-1000 powder. After a



Scheme 1. Schematic illustration of the biocatalytic process in the continuous flow reactor.

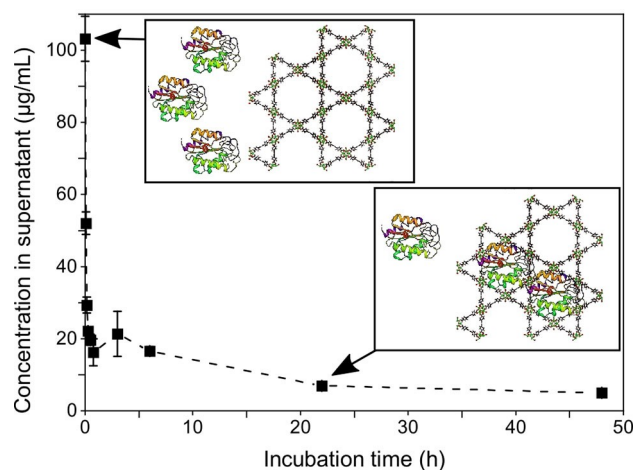


Figure 1. Esterase loading kinetics. 0.5 mg of NU-1000 was incubated with 0.5 mL of an esterase solution in TBS (Tris-buffered saline) (150 mM Tris, 150 mM NaCl, pH 7.4) with a $100 \mu\text{g mL}^{-1}$ esterase concentration.

first rapid decrease (down to 40 % of the initial concentration in the first 5 min) the kinetics slow down and reach a value of about 25 % after 10 min. After 4.5 h, 15 % of the initial esterase concentration is still left, and after 46 h a residual value of 8 % is reached. The maximum loading value of $173 \mu\text{g}$ esterase per mg MOF (see Figure S6) corresponds to roughly 1 enzyme in every 8th NU-1000 unit-cell. The results clearly indicate a successful loading of the enzyme into the MOF pores. The loading kinetics are rather similar to that reported for a different, about 1.5 times smaller enzyme, cutinase (MW 22.5 kDa), loaded in the same MOF material.^[22]

To directly image the location of the enzymes within the MOF particles we used a Cy5-labeled esterase (Cy5-AaEST2). After soaking of NU-1000 powder with Cy5-AaEST2, the particles were analyzed by in situ confocal laser scanning microscopy (CLSM, Figure 2). The obtained images allowed to identify an adlayer coated on the outer surface of the MOF particles and strong fluorescence mainly at the ends of the MOF. Towards the center the fluorescence signals were weaker, but there a distinct background inside the NU-1000 rods was clearly evident (Figure 2C). Figure 2A shows a schematic view of the Cy5-AaEST2 loaded into the rods. Notably, the background signals and the fluorescence at the ends of the MOF particles were absent in control experiments carried out with NU-1000 particles, which were first loaded with unlabeled esterase (see Figure 2D and schematic representation Figure 2B). In this case, the CLSM images only showed the adlayer, thus confirming that the background seen in Figure 2A indeed corresponds to Cy5-labelled esterase inside the pores. These findings are in accord with those of Farha and co-workers who demonstrated that a different protein, cutinase is also mainly located inside the NU-1000 particles.^[22]

Prior to the continuous-flow experiments, the hydrolysis of pNP (see Scheme S2) was studied in batch reactors for

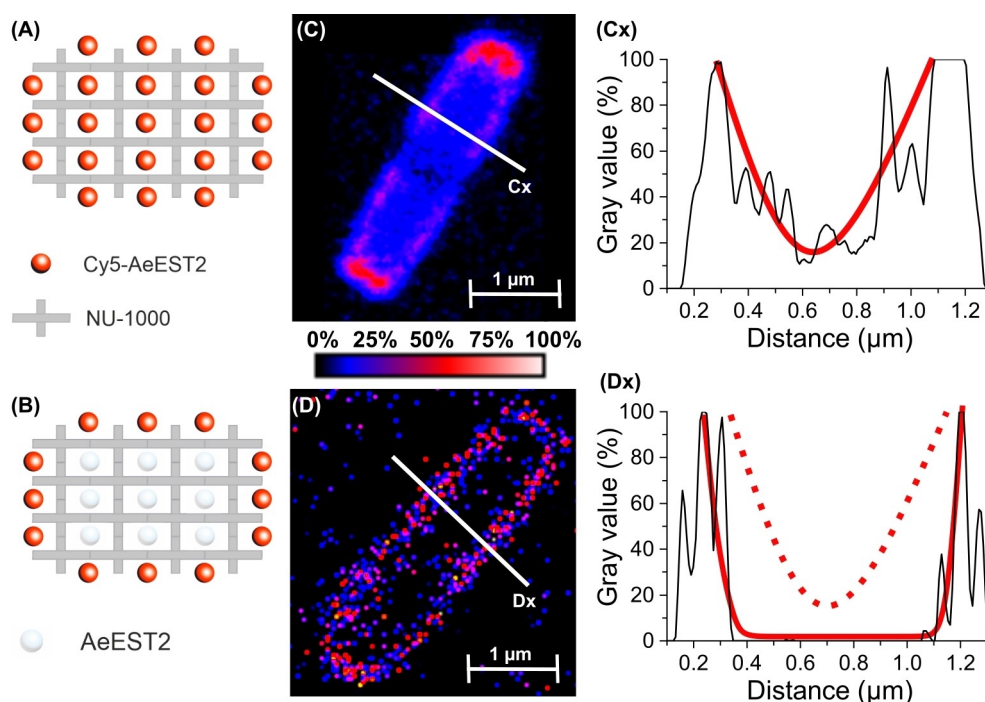


Figure 2. CLSM cross-sectional and schematic images of NU-1000 incubated with a Cy5-labeled esterase solution. First, empty NU-1000 (A/C) was incubated with Cy5-labeled esterase solution for 1 h. As a control NU-1000 was initially loaded with unlabeled esterase (B/D) and subsequently incubated with Cy5-labeled esterase solution for 1 h. The fluorescence signals quantified in grayscale values, indicating the presence of the Cy5-labeled esterase in the images (C) and (D), were measured along the lines Cx and Dx. The letters of the lines Cx and Dx correspond to the images (Cx) and (Dx). In (Cx) and (Dx) the red curves specify the trend lines of the gray values. The red dotted curve in (Dx) shows represents the trend line of (Cx).

free esterase in solution and for suspended Enzyme@MOF crystals (details see Supporting Information). For both cases the results revealed a typical Michaelis–Menten behavior (see Figure 3) with parameters $K_m=86.7 \mu\text{M}$ and $k_{\text{cat}}=$

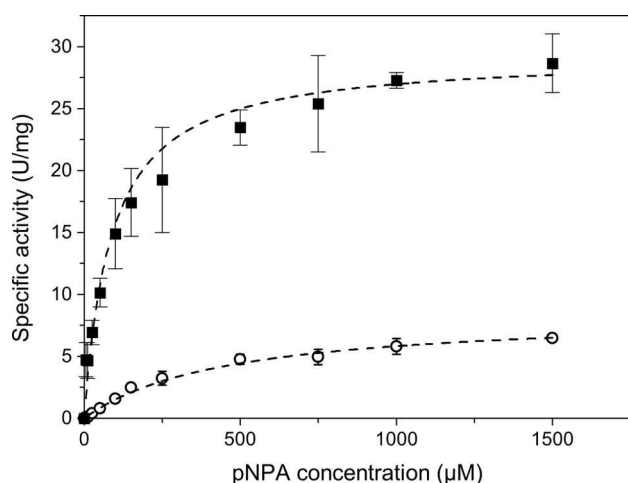


Figure 3. Michaelis–Menten kinetics of free (squares) and immobilized esterase (circles) for the substrate pNPA. Kinetic studies were determined with $0.071 \mu\text{g mL}^{-1}$ of free esterase in solution and $0.56 \mu\text{g mL}^{-1}$ Esterase@NU-1000 with 5–1500 μM pNP. The kinetic constants were determined by fitting a Michaelis–Menten equation $v = v_{\text{max}}[S]/(K_m + [S])$ to the experimental data.

17.1 s^{-1} for the free enzymes and $K_m=457 \mu\text{M}$ and $k_{\text{cat}}=5 \text{ s}^{-1}$ for the encapsulated enzyme. The about 3-fold reduction of k_{cat} as compared to the free enzyme indicates a lower overall activity of the encapsulated esterase, while the more than 5-fold higher K_m points towards a weaker affinity of the reactant to the enzyme inside the MOF pores.

All-atom explicit solvent molecular dynamics (MD) simulations were performed to explore the structural changes in Esterase upon encapsulation in the pores of NU-1000 (see Supporting Information for more details). We have observed a stable form of the Esterase with a 10% increase in the radius of gyration of immobilized NU-1000 as shown in Figure 4. This partial unfolding is accompanied by a slight opening of the active site of the enzyme (see Figure S3). These theoretical results suggest that the reduced activity of the encapsulated enzyme seen in the flow reactor experiments results from slight distortions of the esterase's tertiary structure caused by embedding into the pores of NU-1000 (see Scheme S1).

For the continuous flow experiments, 5 mg NU-1000 were inserted into a HPLC column serving as the reactor. The remaining space was filled with silica, which is completely inert for the reactions investigated here (see Supporting Information). After filling the column, loading with the enzyme was carried out by flowing a solution of AaEST2 through the reactor, reaching a maximum loading of $170 \mu\text{g}$ enzyme per mg MOF, almost identical to the values obtained in the batch experiments.

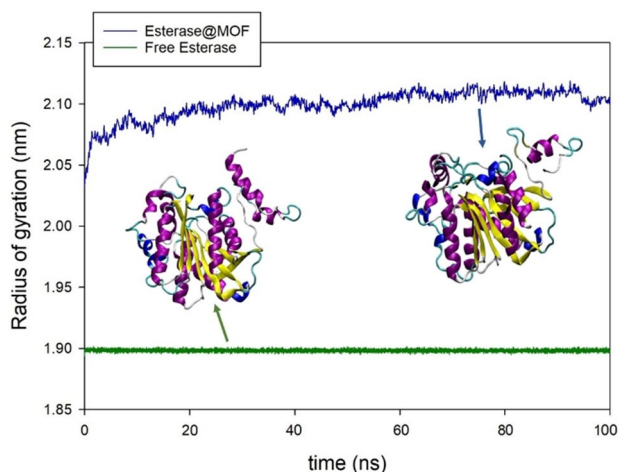


Figure 4. Time evolution of the radius of gyration for free (green) and confined (blue) Esterase, which demonstrate the existence of a stable, but slightly larger conformation of the enzyme in the MOF. The insets illustrate an opening in the active site (discussed in the Supporting Information).

To demonstrate the continuous catalytic reaction a loading of $18.5 \mu\text{g mg}^{-1}$ was used to avoid possible mass transfer limitations. The column was filled with empty MOF particles and loaded with enzyme afterwards, because the filling process is done in pure ethanol, which could negatively affect the enzyme. In addition, when using very precious enzymes, this strategy is more efficient, since there is always loss of MOF particles when filling the column. The continuous flow experiments were carried out by pumping a 3 mM pNPA solution in TBS (Tris-buffered saline) (150 mM Tris, 150 mM NaCl, pH 7.4) through the column with stepwise decreasing flowrates, and the concentration of the product was determined by UV/Vis at 405 nm (Figure 5). At

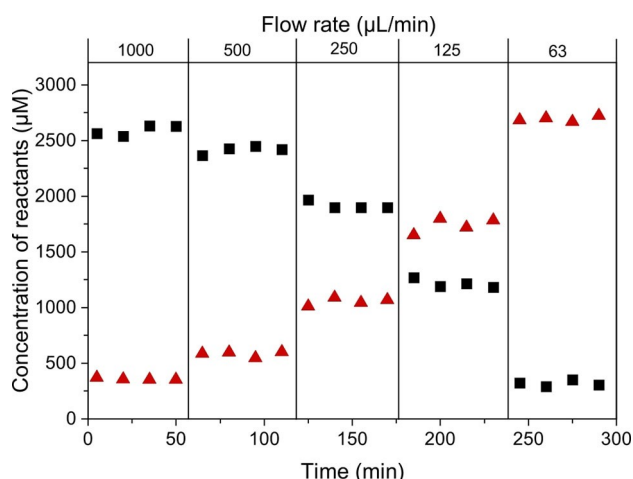


Figure 5. A continuous flow catalytic reaction conducted within a micro flow reactor filled with 5 mg Enzyme@MOF crystals. A feed solution with 3 mM pNPA (black squares) was pumped through a column with stepwise decreasing flowrates. The concentration of the product pNP (red triangles) was measured at 405 nm.

the highest flow rate the reactor reached a yield of 12% under steady state conditions. For lower flow rates and therefore higher contact times the yield increased up to a final value of 90% for the lowest flow rate of $0.0625 \text{ mL min}^{-1}$ after reaching steady state conditions. The stepwise increasing product concentration for increasing residence times of the solution indicated that the investigated enzymatic reaction is kinetically controlled and did not reach its final equilibrium state. Figure 6 summarizes the resulting product concentrations in the effluent after reaching steady state conditions at different flow rates for experiments using various substrate concentrations. For all feed concentrations the product concentrations under steady state conditions reached approximately the same values of 350, 550 and $1000 \mu\text{M}$ at the highest flow rates of 1, 0.5 and 0.25 mL min^{-1} , respectively.

For a quantitative comparison with other cases of continuous flow reactors with enzymes embedded in protecting host materials we considered the STY values at 50%

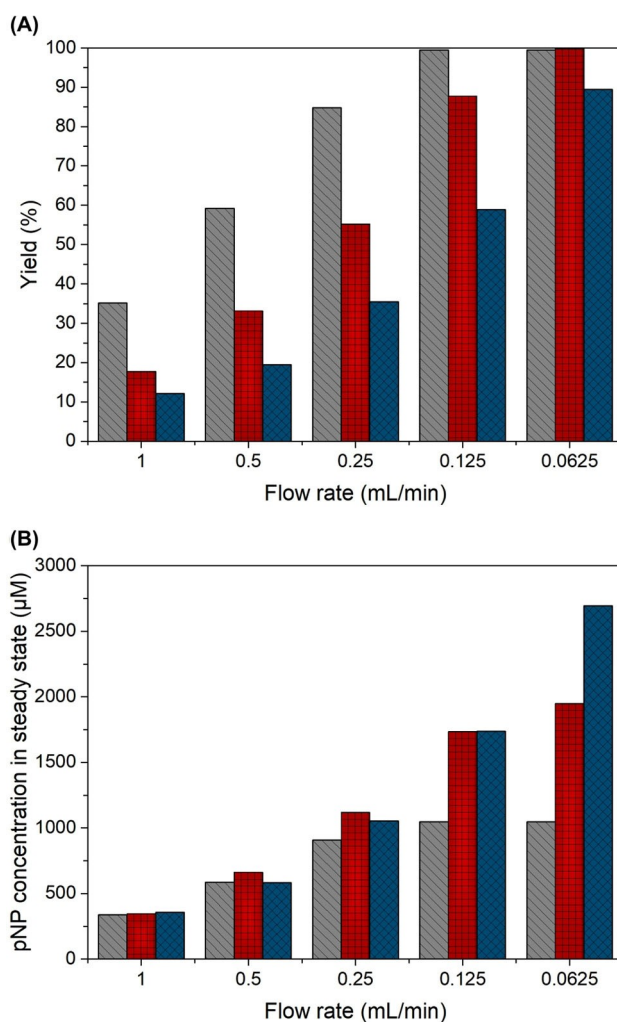


Figure 6. Yields (A) and pNP concentrations (B) in the effluent after reaching steady state conditions in a column filled with 5 mg Esterase@NU-1000 for different flow rates and feed concentrations of 1 mM pNPA (grey), 2 mM pNPA (red) and 3 mM pNPA (blue).

conversion yields. To reach a conversion yield of 50 % the substrate concentration in the feed solution was successively increased. With the maximum loading of 170 μg enzyme per mg MOF and a flow rate of 1 mL min^{-1} , the feed concentration needed was 8 mM pNPA. Thereby, our system reached a STY of 1432 $\text{g L}^{-1} \text{h}^{-1}$ and a productivity of 6.9 g product per g MOF per h. Ma et al. used a different esterase (rPPE01W187H) immobilized in an epoxy-functionalized resin. In their continuous flow experiments (deacetylation of racemic AcO-CPA) a STY of 139.2 $\text{g L}^{-1} \text{h}^{-1}$ for a conversion of 50 % was achieved.^[33] This value is substantially, by an order of magnitude, lower than the STY observed here for the Enzyme@MOF system. We therefore conclude that the activity of MOF-embedded enzymes can be higher than an enzyme immobilized on a functionalized resin^[28] or other solid supports such as zeolites, kaolin, montmorillonite and ion exchange resins.^[37] The turnover frequency (TOF) of the Enzyme@MOF flow reactor at a yield of 50 % amounted to 1.74 $\mu\text{mol pNP}$ per μmol esterase per s, which can be compared to the corresponding value for the batch experiments, 1.65 $\mu\text{mol} \mu\text{mol}^{-1} \text{s}^{-1}$. Even though the flowrates in the reactor led to very short contact times (1.5–24 s) of substrate there does not seem to be a diffusion limitation in comparison to batch experiments. This finding reveals a high quality of the MOF packing.

The Enzyme@MOF in the reactor showed excellent stability in long term performance in aqueous solution. They were in contact with 57 600 times their volume in the column per day for several weeks. During this time period, no obvious inactivation of the embedded protein was observed, while for the free enzyme a reduction to 50 % was observed already after 5.2 days when stored at 7 °C. Furthermore, the Enzyme@MOF in the continuous reactor achieved 10 times higher STY than comparable immobilized enzyme reactors.

Importantly, the increased stability of the MOF-embedded enzyme also allowed the use organic solvents. With the same Enzyme@MOF reactor we were able to continuously synthesize isoamyl acetate, banana flavor ester, using acetonitrile as a solvent (see Figure 7). After an initial decrease a stable conversion with a product concentration of about 6 mM was reached, demonstrating that the immobilized enzyme is suited also for organic solvents. For a proof-of-concept experiment which needs to be optimized, a STY of 113 $\text{g L}^{-1} \text{h}^{-1}$ and a productivity of 0.54 $\text{g g}^{-1} \text{h}^{-1}$ are very competitive with performance metrics in aqueous solutions.^[33]

In summary, we demonstrated the fabrication of continuous-flow biocatalysts for reactions in aqueous and organic solvents based on embedding an enzyme into a highly stable reticular framework. We were able to load the esterase AaEST2 into the MOF NU-1000 by simple indiffusion. We would like to point out that this preparation of the Enzyme@MOF flow reactor is very time and cost effective and thus outperforms other enzyme immobilization strategies used for continuous processes like cross-linking and binding to a (porous) carrier.^[33] A careful analysis of the hydrolysis of 4-nitrophenyl acetate using batch and continuous flow setups gave a thorough understanding of the mechanism of the reaction. In contrast to expectation, the

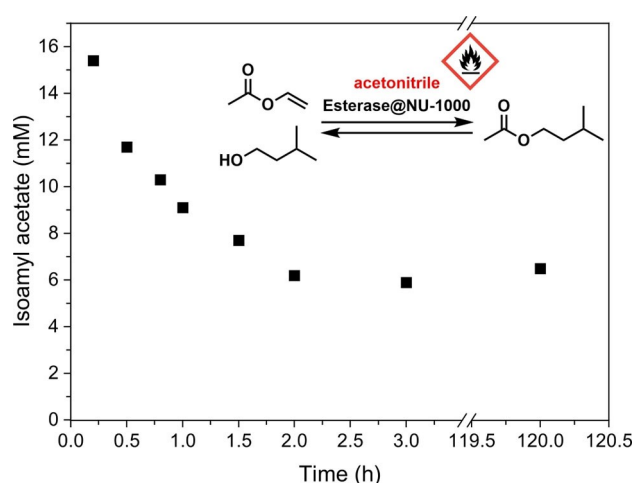


Figure 7. Proof-of-concept continuous flow synthesis of isoamyl acetate in acetonitrile. The reactor was filled with 5 mg Enzyme@MOF crystals with a loading of 170 mg g^{-1} . The feed solution, 2 M 3-methyl-1-butanol and 4 M vinyl acetate, was pumped with a flow rate of 0.05 mL min^{-1} .

total STY is not limited by the diffusivity of the reactants and products, but by the activity of the embedded esterase. A careful analysis of our batch experiments reveals that the activity of Enzyme@MOF amounts to about 30 % of that of free enzyme, a fairly high value considering the distortion of the catalytically active protein upon embedding into the MOF. For applications in real-world systems, it has to be considered that this reduction of activity is compensated by the increase in stability of the enzymes, including the possibility to use organic solvents, and the straightforward separation of the catalyst from the products.

In the future, we will use the simulation workflow described above to scan different types of MOF linkers in silico^[38] and investigate their effect on the conformation of embedded proteins. Such studies will allow further optimizing the enzymatic activity and stability within such continuous-flow Enzyme@MOF reactors.

Acknowledgements

T.H., E.S., W.W., and C.W. acknowledge support from the Deutsche Forschungsgemeinschaft (DFG, German Research Foundation) under the Germany Excellence Strategy via the Excellence Cluster 3D Matter Made to Order (grant no. EXC-2082/1-390761711). Additional financial support came from the Helmholtz program “Materials Systems Engineering” under the topic “Adaptive and Bioinspired Materials Systems”. Open Access funding enabled and organized by Projekt DEAL.

Conflict of Interest

The authors declare no conflict of interest.

Data Availability Statement

The data that support the findings of this study are available in the Supporting Information of this article.

Keywords: Biocatalysis · Continuous Reactors · Enzymes · Immobilization · Metal–Organic Frameworks

- [1] R. A. Sheldon, P. C. Pereira, *Chem. Soc. Rev.* **2017**, *46*, 2678–2691.
- [2] K. S. Rabe, J. Müller, M. Skoupi, C. M. Niemeyer, *Angew. Chem. Int. Ed.* **2017**, *56*, 13574–13589; *Angew. Chem.* **2017**, *129*, 13760–13777.
- [3] R. A. Sheldon, A. Basso, D. Brady, *Chem. Soc. Rev.* **2021**, *50*, 5850–5862.
- [4] S. Wu, R. Snajdrova, J. C. Moore, K. Baldenius, U. T. Bornscheuer, *Angew. Chem. Int. Ed.* **2021**, *60*, 88–119; *Angew. Chem.* **2021**, *133*, 89–123.
- [5] S. Simić, E. Zukić, L. Schmermund, K. Faber, C. K. Winkler, W. Kroutil, *Chem. Rev.* **2022**, *122*, 1052–1126.
- [6] W. Aehle, *Enzymes in Industry: Production and Applications*, Wiley, Hoboken, **2007**.
- [7] K. Sumida, D. L. Rogow, J. A. Mason, T. M. McDonald, E. D. Bloch, Z. R. Herm, T.-H. Bae, J. R. Long, *Chem. Rev.* **2012**, *112*, 724–781.
- [8] J.-R. Li, J. Sculley, H.-C. Zhou, *Chem. Rev.* **2012**, *112*, 869–932.
- [9] H.-C. Zhou, J. R. Long, O. M. Yaghi, *Chem. Rev.* **2012**, *112*, 673–674.
- [10] K. Hirai, J. Reboul, N. Morone, J. E. Heuser, S. Furukawa, S. Kitagawa, *J. Am. Chem. Soc.* **2014**, *136*, 14966–14973.
- [11] P. Horcajada, T. Chalati, C. Serre, B. Gillet, C. Sebrie, T. Baati, J. F. Eubank, D. Heurtaux, P. Clayette, C. Kreuz, J.-S. Chang, Y. K. Hwang, V. Marsaud, P.-N. Bories, L. Cynober, S. Gil, G. Férey, P. Couvreur, R. Gref, *Nat. Mater.* **2010**, *9*, 172–178.
- [12] K. Liang, J. J. Richardson, C. J. Doonan, X. Mulet, Y. Ju, J. Cui, F. Caruso, P. Falcaro, *Angew. Chem. Int. Ed.* **2017**, *56*, 8510–8515; *Angew. Chem.* **2017**, *129*, 8630–8635.
- [13] R. Riccò, W. Liang, S. Li, J. J. Gassensmith, F. Caruso, C. Doonan, P. Falcaro, *ACS Nano* **2018**, *12*, 13–23.
- [14] W. Liang, P. Wied, F. Carraro, C. J. Sumby, B. Nidetzky, C.-K. Tsung, P. Falcaro, C. J. Doonan, *Chem. Rev.* **2021**, *121*, 1077–1129.
- [15] B. Somturk, M. Hancer, I. Ocoy, N. Özdemir, *Dalton Trans.* **2015**, *44*, 13845–13852.
- [16] Q. Wang, X. Zhang, L. Huang, Z. Zhang, S. Dong, *Angew. Chem. Int. Ed.* **2017**, *56*, 16082–16085; *Angew. Chem.* **2017**, *129*, 16298–16301.
- [17] Q. Zhu, W. Zhuang, Y. Chen, Z. Wang, B. Villacorta Hernandez, J. Wu, P. Yang, D. Liu, C. Zhu, H. Ying, *ACS Appl. Mater. Interfaces* **2018**, *10*, 16066–16076.
- [18] S. Huang, X. Kou, J. Shen, G. Chen, G. Ouyang, *Angew. Chem. Int. Ed.* **2020**, *59*, 8786–8798; *Angew. Chem.* **2020**, *132*, 8868–8881.
- [19] J. Liu, J. Liang, J. Xue, K. Liang, *Small* **2021**, *17*, 2100300.
- [20] K. Hernandez, R. Fernandez-Lafuente, *Enzyme Microb. Technol.* **2011**, *48*, 107–122.
- [21] R. A. Sheldon, *Biochem. Soc. Trans.* **2007**, *35*, 1583–1587.
- [22] P. Li, J. A. Modica, A. J. Howarth, E. Vargas, L. P. Z. Moghadam, R. Q. Snurr, M. Mrksich, J. T. Hupp, O. K. Farha, *Chem* **2016**, *1*, 154–169.
- [23] X. Gao, Y. Ding, Y. Sheng, M. Hu, Q. Zhai, S. Li, Y. Jiang, Y. Chen, *ChemCatChem* **2019**, *11*, 2828–2836.
- [24] Y. Zhong, L. Yu, Q. He, Q. Zhu, C. Zhang, X. Cui, J. Zheng, S. Zhao, *ACS Appl. Mater. Interfaces* **2019**, *11*, 32769–32777.
- [25] D. Tian, X. Zhang, H. Shi, L. Liang, N. Xue, J.-H. Wang, H. Yang, *J. Am. Chem. Soc.* **2021**, *143*, 16641–16652.
- [26] V. Stavila, R. Parthasarathi, R. W. Davis, F. El Gabaly, K. L. Sale, B. A. Simmons, S. Singh, M. D. Allendorf, *ACS Catal.* **2016**, *6*, 55–59.
- [27] M. Ali, E. Pervaiz, T. Noor, O. Rabi, R. Zahra, M. Yang, *Int. J. Energy Res.* **2021**, *45*, 1190–1226.
- [28] S. Mosleh, M. R. Rahimi, M. Ghaedi, K. Dashtian, S. Hajati, *RSC Adv.* **2016**, *6*, 63667–63680.
- [29] P. Elumalai, N. Elrefaei, W. Chen, M. Al-Rawashdeh, S. T. Madrahimov, *Catalysts* **2020**, *10*, 1159.
- [30] a) D. E. Agafonov, K. S. Rabe, M. Grote, Y. Huang, M. Sprinzl, *FEBS Lett.* **2005**, *579*, 2082–2086; b) M. Maier, C. P. Radtke, J. Hubbuch, C. M. Niemeyer, K. S. Rabe, *Angew. Chem. Int. Ed.* **2018**, *57*, 5539; *Angew. Chem.* **2018**, *130*, 5638.
- [31] G. Manco, E. Adinolfi, F. M. Pisani, G. Ottolina, G. Carrea, M. Rossi, *Biochem. J.* **1998**, *332*, 203–212.
- [32] J. E. Mondloch, W. Bury, D. Fairen-Jimenez, S. Kwon, E. J. DeMarco, M. H. Weston, A. A. Sarjeant, S. T. Nguyen, P. C. Stair, R. Q. Snurr, O. K. Farha, J. T. Hupp, *J. Am. Chem. Soc.* **2013**, *135*, 10294–10297.
- [33] B.-D. Ma, H.-L. Yu, J. Pan, J.-H. Xu, *Biochem. Eng. J.* **2016**, *107*, 45–51.
- [34] P. De Santis, L.-E. Meyer, S. Kara, *React. Chem. Eng.* **2020**, *5*, 2155–2184.
- [35] T. Islamoglu, K. Otake, P. Li, C. T. Buru, A. W. Peters, I. Akpınar, S. J. Garibay, O. K. Farha, *CrystEngComm* **2018**, *20*, 5913–5918.
- [36] J. Liu, Z. Li, X. Zhang, K. Otake, L. Zhang, A. W. Peters, M. J. Young, N. M. Bedford, S. Letourneau, D. J. Mandia, *ACS Catal.* **2019**, *9*, 3198–3207.
- [37] R. Scherer, J. V. Oliveira, S. Pergher, D. de Oliveira, *Mater. Res.* **2011**, *14*, 483–492.
- [38] R. Haldar, A. Mazel, M. Krstić, Q. Zhang, M. Jakoby, I. A. Howard, B. S. Richards, N. Jung, D. Jacquemin, S. Diring, W. Wenzel, F. Odobel, C. Wöll, *Nat. Commun.* **2019**, *10*, 2048.

Manuscript received: December 16, 2021

Accepted manuscript online: February 8, 2022

Version of record online: March 9, 2022